Linear Matching Method on the evaluation of plastic and creep behaviours for bodies subjected to cyclic thermal and mechanical loading

Haofeng Chen[*,†] and Alan R.S. Ponter

Department of Engineering, University of Leicester, Leicester, LE1 7RH, UK

SUMMARY

This paper extends the previous Linear Matching Method (LMM) to allow for the evaluation of plastic, creep and ratchet strains of structures subjected to a general load condition in a steady cyclic state. The constant and varying residual stress fields associated with differing mechanisms as well as the steady cyclic stress state of the whole component are obtained for further structural design and assessment. The total strain range for use in fatigue assessment, including the effects of creep and plastic strains are obtained. A typical example of 3D holed plate subjected to cyclic thermal load and constant mechanical load are assessed here in detail to verify the applicability of the proposed numerical technique. The LMM results in the paper are compared with those by ABAQUS step-by-step inelastic analyses and demonstrate that LMM have both the advantages of programming methods and the capacity to be implemented easily within a commercial finite element code, in this case, ABAQUS. The LMM provides a general-purpose technique for the evaluation of creep/ fatigue interaction.

KEY WORDS: linear matching, plastic, creep, ratchetting, steady cyclic state

1. INTRODUCTION

The operating lifetime of components subjected to cyclic thermal and mechanical loading are normally limited by the mechanisms of low-cycle fatigue, creep fatigue interaction and excessive plastic deformation [1, 2]. The evaluation of creep/fatigue interaction and other failure mechanisms

[*] Correspondence to: Haofeng Chen, Department of Engineering, University of Leicester, Leicester, LE1 7RH, UK
[†] E-mail: hfc3@le.ac.uk

of structures with variable repeated loading is a significant problem and has attracted the attentions of many researchers [3-9].

One of the most successful of such methods, the Linear Matching Method (LMM) [10-12] has been applied with considerable rigor to cyclic loading problems where the residual stress field remains constant. This includes the evaluation of classical limit loads, shakedown limits, creep ruptures and rapid cycle creep solutions. The LM method has also been extended to cases where the residual stress field changes during a cyclic state [12-15]. This includes the assessment of the plastic strain amplitude and ratchet limit associated with reverse plasticity mechanisms when the load history is in excess of shakedown but less than a ratchet limit. In these circumstances there are two properties required in low temperature design and life assessment. The amplitude of plastic strain provides information concerning fatigue crack initiation in low cycle fatigue and the capacity of the body to withstand additional constant mechanical load indicates the proximity to a ratchet limit. In [14], the LMM has been extended to characterise both the strain amplitude and the proximity to a ratchet limit, based upon a new minimum theorem [13].

In practice, components operate at high temperature within the creep range both within shakedown and for load ranges in excess of shakedown. Typically, in power plant, a creep dwell periods exist where the temperature of some proportion of the structure lies within the creep range. For some components, e.g. heat exchangers, the mechanical loads can be relatively small but the thermal stresses can be significantly in excess of yield. In such circumstances creep strains occur, and this results in the relaxation of initially high stresses as creep strains replaces elastic strains. Lifetime integrity may then be limited not only by low cycle fatigue but the damaging effects of the creep strains produced during creep relaxation. The evaluation of the creep relaxation, the determination of the accumulated creep strain, the varying flow stress and the corresponding elastic follow-up factors during dwell period are very important components of life assessment methods [1]. The work of [12] gave a general study of the application of the LMM to the various stages of life assessment in R5 [1] as the beginning point. It is anticipated that such methods may provide a viable alternative to rule-based methods currently used, providing more accurate and less conservative predictions.

However, the assessment procedures in [12, 15, 16] for creep/fatigue interaction only involve the cyclic thermal stress. Only two load instances were considered in [15, 16] for method 1, which is

suggested as the basis of a general purpose method for use in life assessment. For a general case of arbitrary loading, a more general method should be developed.

The evaluation of ratchet strains is also important in engineering practice. In nuclear plant structures, e.g. a typical AGR superheater headers in [17-19], the load conditions are such that the ratchetting may occur. The accumulated ratchet strain may be acceptable due to the limited number of load cycles. In such cases, the determination of ratchet strains is significant.

The primary objective of this paper is to investigate the possibility of extending the current LMM to allow for the evaluation of plastic, creep and ratchet strains of structures subjected to a general load condition in a steady cyclic state. The problem of a plate with a central circular hole is discussed, subjected to cyclic thermal load and constant mechanical load. In this paper, in order to demonstrate the applicability of the proposed LMM, all the LMM solutions are compared with step-by-step inelastic analysis results.

2. DEFINITION OF THE PROBLEM

Consider the following problem. A structure is subjected to a cyclic history of varying temperature $\lambda_\theta \theta(x_i,t)$ within the volume of the structure and varying surface loads $\lambda_P P_i(x_i,t)$ acting over part of the structure's surface S_T. The variation is considered over a typical cycle $0 \le t \le \Delta t$. Here λ_θ and λ_P denote load parameters, allowing a whole class of loading histories to be considered. On the remainder of the surface S, denoted by S_u, the displacement $u_i = 0$.

Corresponding to these loading histories there exists a linear elastic solution history;

$$\hat{\sigma}_{ij}^{e} = \lambda_\theta \hat{\sigma}_{ij}^{\theta} + \lambda_P \hat{\sigma}_{ij}^{P} \tag{1}$$

where $\hat{\sigma}_{ij}^{\theta}$ and $\hat{\sigma}_{ij}^{P}$ are the solutions corresponding to $\theta(x_i,t)$ and $P_i(x_i,t)$, respectively.

Consider a typical cycle $0 \le t \le \Delta t$. The cyclic solution may be expressed in terms of three components, the elastic solution, a transient solution accumulated up to the beginning of the cycle and a residual solution that represents the remaining changes within the cycle. The linear elastic solution (i.e. $\dot{\varepsilon}_{ij}^{p}$=0) is denoted by $\hat{\sigma}_{ij}^{e}$. The general form of the stress solution for the cyclic problems involving changing and constant residual stress fields is given by

$$\sigma_{ij}(x_i,t) = \hat{\sigma}_{ij}^{e}(x_i,t) + \overline{\rho}_{ij}(x_i) + \rho_{ij}^{r}(x_i,t) \tag{2}$$

where $\overline{\rho}_{ij}$ denotes a constant residual stress field in equilibrium with zero surface traction on S_T and corresponds to the residual state of stress at the beginning and end of the cycle. The history ρ^r_{ij} is the change in the residual stress during the cycle and satisfies;

$$\rho^r_{ij}(x_i,0) = \rho^r_{ij}(x_i,\Delta t) = 0 \tag{3}$$

Hence, the stresses and strain rates will asymptote to a cyclic state where;

$$\sigma_{ij}(t) = \sigma_{ij}(t+\Delta t),\ \dot{\varepsilon}_{ij}(t) = \dot{\varepsilon}_{ij}(t+\Delta t) \tag{4}$$

It is worth noting that the arguments in this section do not explicitly call on the properties of perfect plasticity and are therefore common to all cyclic states associated with inelastic material behaviour.

Both the Linear Matching Method and R5 [1] are concerned with properties of this cyclic solution, based upon a sequence of constitutive assumptions, drawing on the data base of materials data. Whereas R5 [1] relies significantly on rule-based calculations based on the linear elastic solution, the Linear Matching Method produces direct calculations of various performance indicators as derived from simplified continuum problems.

3. MODES OF BEHAVIOUR

If we define λ^E, λ^S, λ^P as the elastic limit multiplier, shakedown limit multiplier and ratchet limit multiplier respectively, the four major mechanisms including elasticity, shakedown, reverse plasticity and ratchetting can be described as follows:

E - Elastic region - $0 \le \lambda \le \lambda^E$, where $f(\hat{\sigma}^e_{ij}) \le 0$ throughout V

S – Shakedown - $\lambda^E \le \lambda \le \lambda^S$, where $f(\hat{\sigma}^e_{ij} + \overline{\rho}_{ij}) \le 0$ and $\overline{\rho}_{ij}$ is a constant residual stress field

P – Reverse Plasticity - $\lambda^S \le \lambda \le \lambda^P$, where $f(\hat{\sigma}^e_{ij} + \overline{\rho}_{ij} + \rho^{pr}_{ij}) \le 0$, and $\rho^{pr}_{ij}(t)$ is a changing residual stress field, derived from a plastic strain rate history $\dot{\varepsilon}^{pr}_{ij}$ that satisfies the *zero growth* condition $\int_0^{\Delta t} \dot{\varepsilon}^{pr}_{ij} dt = 0$ everywhere in V.

R – Ratchetting - $\lambda^P \le \lambda$, where $f(\hat{\sigma}^e_{ij} + \overline{\rho}_{ij} + \rho^{pr}_{ij}) \le 0$, and $\rho^{pr}_{ij}(t)$ is a changing residual stress field, derived from a plastic strain rate history $\dot{\varepsilon}^{pr}_{ij}$ that satisfies the *growth* condition

$\int_0^{\Delta t} \dot{\varepsilon}_{ij}^{pr} dt = \Delta\varepsilon_{ij}^{pr}$ where $\Delta\varepsilon_{ij}^{pr}$ is a compatible accumulated strain giving rise to non-zero displacement increment Δu_i^{pr}.

The behaviour progresses, for increasing λ, from the most benign, the E region, to the most serious, the R region. At the transition values of λ we reach the position that, for increasing λ there no longer exists a solution of the form that characterised the exiting region. Hence, when λ increases above λ^E, somewhere $f(\lambda\hat{\sigma}_{ij}) > 0$. Similarly when λ increases above λ^S, there no longer exists a constant residual stress field $\overline{\rho}_{ij}$ so that $f(\lambda\hat{\sigma}_{ij} + \overline{\rho}_{ij}) \le 0$ everywhere. At the same time, if $\lambda > \lambda^S$ then $f(\lambda\hat{\sigma}_{ij} + \overline{\rho}_{ij}) > 0$ somewhere within the volume V, for all possible $\overline{\rho}_{ij}$.

In the above formulations, if we only consider the plastic behaviour of the component, *f* is the function associated with the material yield surface. In the steady cyclic state, if the creep relaxation occurs during the dwell period at some load instances, the function *f* should be adjusted by the creep flow stress which depends on the creep strain rate.

4. MINIMUM THEOREM FOR CYCLIC STEADY STATE SOLUTION

Consider the functional where λ is regarded as prescribed

$$I(\dot{\varepsilon}_{ij}^c, \lambda) = \int_V \int_0^{\Delta t} (\sigma_{ij}^c - \lambda\hat{\sigma}_{ij})\dot{\varepsilon}_{ij}^c dt dV \tag{5}$$

where $\dot{\varepsilon}_{ij}^c$ is subject to the following conditions;

$$\dot{\varepsilon}_{ij}^{cT} = C\dot{\rho}_{ij}^c + \dot{\varepsilon}_{ij}^c, \tag{6}$$

where $\dot{\varepsilon}_{ij}^{cT}$ is compatible and $\Delta\dot{\varepsilon}_{ij}^c = \int_0^{\Delta t} \dot{\varepsilon}_{ij}^c dt$ is also compatible,

In addition there exists a $\overline{\rho}$ so that $f(\lambda\hat{\sigma}_{ij} + \rho_{ij}^c(t) + \overline{\rho}_{ij}) \le 0$ (7)

Then $I(\dot{\varepsilon}_{ij}^c, \lambda) \ge I(\dot{\varepsilon}_{ij}^s, \lambda)$ (8)

where $\dot{\varepsilon}_{ij}^s$ is the exact solution.

Note: Inclusion of $\rho_{ij}^{c}(t)$ and $\bar{\rho}_{ij}$ in I does not change its value. Hence in the following we use;

$$I(\dot{\varepsilon}_{ij}^{c},\lambda)=\int_{V}\int_{0}^{\Delta t}\left\{\sigma_{ij}^{c}-(\lambda\hat{\sigma}_{ij}+\rho_{ij}(t))\dot{\varepsilon}_{ij}^{c}\right\}dtdV \tag{9}$$

where $\rho_{ij}(t)=\bar{\rho}_{ij}+\rho_{ij}^{r}$, and $\rho_{ij}(0)=\bar{\rho}_{ij}$. For I given by (9), inequality (8) still holds.

5. PROBLEM FOR PLASTIC STRAINS OCCURRING AT N DISCRETE TIMES

We essentially adopt the same procedure as [13, 14], and develop a Linear Matching Method that reduces I for each iteration.

We assume that plastic or creep strains occur at N instants, t_1, t_2 ….. t_N, where t_n correspond to a sequence of points in the cyclic history. Hence $\Delta\varepsilon_{ij}^{c}=\sum_{n=1}^{N}\Delta\varepsilon_{ij}^{n}$ where $\Delta\varepsilon_{ij}^{n}$ is the increment of plastic or creep strain that occurs at time t_n. Hence we may write the following approximation for I;

$$I(\dot{\varepsilon}_{ij}^{c},\lambda)=\sum_{n=1}^{N}I^{n} \tag{10}$$

where $$I^{n}(\Delta\varepsilon_{ij}^{n},\lambda,\rho(t_n))=\int_{V}\left\{\sigma_{ij}^{n}\Delta\varepsilon_{ij}^{n}-(\lambda\hat{\sigma}_{ij}^{e}(t_n)+\rho(t_n))\Delta\varepsilon_{ij}^{n}\right\}dV \tag{11}$$

$$\Delta\varepsilon_{ij}^{Tn}=C\Delta\rho_{ij}^{n}+\Delta\varepsilon_{ij}^{n}, \tag{12}$$

where $\Delta\varepsilon_{ij}^{Tn}$ compatible and $\Delta\rho_{ij}^{n}$ satisfies equilibrium.

Note that $$\rho_{ij}(t_n)=\bar{\rho}_{ij}+\sum_{l=1}^{n}\Delta\rho_{ij}^{l} \tag{13}$$

The solution of (12) is equivalent to minimising $\int_{V}U(\Delta\varepsilon_{ij}^{Tn}-\Delta\varepsilon_{ij}^{n})dV$ where,

$$U(\Delta\varepsilon_{ij}^{Tn}-\Delta\varepsilon_{ij}^{n})=\tfrac{1}{2}C^{-1}(\Delta\varepsilon_{ij}^{Tn}-\Delta\varepsilon_{ij}^{n})(\Delta\varepsilon_{kl}^{Tn}-\Delta\varepsilon_{kl}^{n}) \tag{14}$$

Hence the problem becomes that of minimising;

$$\bar{I}^{n}(\Delta\varepsilon_{ij}^{n},\Delta\varepsilon_{ij}^{Tn},\lambda,\rho(t_n))=\int_{V}\left\{\Omega-(\lambda\hat{\sigma}_{ij}+\rho(t_n))\Delta\varepsilon_{ij}^{n}\right\}dV \tag{15}$$

with respect to $\Delta\varepsilon_{ij}^{Tn}$ and $\Delta\varepsilon_{ij}^{n}$ where

$$\Omega = \sigma_{ij}^{n}\Delta\varepsilon_{ij}^{n} + U \tag{16}$$

6. LINEAR MATCHING METHOD SOLUTION

The minimisation problem (14) and (15) is identical in form to the minimisation problem in [13, 14]. Hence the process is as follows for isotropic elastic properties and a von Mises yield condition. The latter will be replaced by creep flow stress if only creep relaxation occurs at the load instance. Assume we have an initial estimate of $\Delta\varepsilon_{ij}^{n} = \Delta\varepsilon_{ij}^{ni}$. Define shear modulus by linear matching

$$\sigma_0 = 2\overline{\mu}_{ni}\overline{\varepsilon}(\Delta\varepsilon_{ij}^{ni}) \tag{17}$$

where σ_0 is the von Mises yield stress or creep flow stress.

Solve the following linear problem;

$$\Delta\varepsilon_{ij}^{Tf\,\prime} = \frac{1}{2\mu}\Delta\rho_{ij}^{nf\,\prime} + \Delta\varepsilon_{ij}^{nf\,\prime}, \quad \Delta\varepsilon_{kk}^{Tf} = \frac{1}{3K}\Delta\rho_{kk}^{nf} \tag{18}$$

$$\Delta\varepsilon_{ij}^{nf\,\prime} = \frac{1}{2\overline{\mu}_{ni}}\left\{\lambda\hat{\sigma}_{ij}^{e}(t_n) + \rho_{ij}(t_{n-1}) + \Delta\rho_{ij}^{nf}\right\}' \tag{19}$$

where

$$\rho_{ij}(t_{n-1}) = \rho_{ij}(t_0) + \Delta\rho_{ij}^{1} + \Delta\rho_{ij}^{2} + ... + \Delta\rho_{ij}^{n-1},\ \rho_{ij}(t_0) = \overline{\rho}_{ij} \tag{20}$$

7. ITERATION PROCEDURES

In order to simplify the calculation, the entire iterative procedure includes a number of cycles. Each cycle contains n iterations associated with n load instances. The first iteration is to evaluate the changing residual stress $\Delta\rho_{ij}^{1}$ for the elastic solution $\hat{\sigma}_{ij}^{e}(t_1)$ at the first load instance. We denote $\Delta\rho_{ij}{}_{L}^{K}$ as the calculated changing residual stress for Kth load instance at L cycle of iterations, where K=1,2, … , n and L=1,2, … , m. The whole iterative procedure can be shown as follows:

At cycle 1 of iterations:

Iteration 1: we solve $\Delta\rho_{ij_1}^{\ 1}$ from the elastic solution $\hat{\sigma}_{ij}^{e}(t_1)$ at the first load instance.

Iteration 2: we solve $\Delta\rho_{ij_1}^{\ 2}$ from $\hat{\sigma}_{ij}^{e}(t_2)+\Delta\rho_{ij_1}^{\ 1}$

Iteration n: we solve $\Delta\rho_{ij_1}^{\ n}$ from $\hat{\sigma}_{ij}^{e}(t_n)+\Delta\rho_{ij_1}^{\ 1}+\Delta\rho_{ij_1}^{\ 2}+\cdots+\Delta\rho_{ij_1}^{\ n-1}$

At cycle 2 of iterations:

Iteration n+1: we solve $\Delta\rho_{ij_2}^{\ 1}$ from $\hat{\sigma}_{ij}^{e}(t_1)+\Delta\rho_{ij_1}^{\ 1}+\Delta\rho_{ij_1}^{\ 2}+\cdots+\Delta\rho_{ij_1}^{\ n}$

Iteration n+2: we solve $\Delta\rho_{ij_2}^{\ 2}$ from $\hat{\sigma}_{ij}^{e}(t_2)+\Delta\rho_{ij_1}^{\ 1}+\Delta\rho_{ij_1}^{\ 2}+\cdots+\Delta\rho_{ij_1}^{\ n}+\Delta\rho_{ij_2}^{\ 1}$

Iteration 2n: we solve $\Delta\rho_{ij_2}^{\ n}$ from $\hat{\sigma}_{ij}^{e}(t_n)+\Delta\rho_{ij_1}^{\ 1}+\Delta\rho_{ij_1}^{\ 2}+\cdots+\Delta\rho_{ij_1}^{\ n}+\Delta\rho_{ij_2}^{\ 1}+\Delta\rho_{ij_2}^{\ 2}+\cdots+\Delta\rho_{ij_2}^{\ n-1}$

At cycle m of iterations:

Iteration mn-n+1: we solve $\Delta\rho_{ij_m}^{\ 1}$ from $\hat{\sigma}_{ij}^{e}(t_1)+\sum_{K=1}^{n}\Delta\rho_{ij_1}^{\ K}+\cdots+\sum_{K=1}^{n}\Delta\rho_{ij_{m-1}}^{\ K}$

Iteration mn-n+2: we solve $\Delta\rho_{ij_m}^{\ 2}$ from $\hat{\sigma}_{ij}^{e}(t_2)+\sum_{K=1}^{n}\Delta\rho_{ij_1}^{\ K}+\cdots+\sum_{K=1}^{n}\Delta\rho_{ij_{m-1}}^{\ K}+\Delta\rho_{ij_m}^{\ 1}$

Iteration mn: we solve $\Delta\rho_{ij_m}^{\ n}$ from $\hat{\sigma}_{ij}^{e}(t_n)+\sum_{K=1}^{n}\Delta\rho_{ij_1}^{\ K}+\cdots+\sum_{K=1}^{n}\Delta\rho_{ij_{m-1}}^{\ K}+\sum_{K=1}^{n-1}\Delta\rho_{ij_m}^{\ K}$

If the convergent solutions are obtained at *m*th cycle of iterations, we must have

$$\sum_{K=1}^{n}\Delta\rho_{ij_m}^{\ K}=0 \tag{21}$$

Hence the constant residual stress over the cycle can be calculated by

$$\bar{\rho}_{ij}=\sum_{K=1}^{n}\Delta\rho_{ij_1}^{\ K}+\sum_{K=1}^{n}\Delta\rho_{ij_2}^{\ K}+\cdots+\sum_{K=1}^{n}\Delta\rho_{ij_m}^{\ K} \tag{22}$$

At each iteration, not only the above changing residual stress for n load instances and the constant residual stress over the cycles, the plastic strain amplitudes at load instances or accumulated creep

strains during dwell period are evaluated as well. The total ratchetting strain can be calculated from these plastic and creep strains thereafter, i.e. $\Delta\varepsilon_{ij}^{R} = \sum_{K=1}^{n} \Delta\varepsilon_{ij}^{K}$

8. CREEP FLOW STRESS

In the iteration that evaluates the plastic strain amplitudes [14], σ_0 is adopted as the material yield stress. But when we calculate the accumulated creep strain during the dwell period, σ_0 equals to the creep flow stress $\sigma_0 = \sigma^c$, which is an implicit function of $\Delta\varepsilon_{ij}^{c}$ and $\Delta\rho_{ij}^{c}$.

During the time interval $t_i \le t \le t_i + \Delta t$, where $\tau = t - t_i$, relaxation of stress takes place so that $\sigma_{ij}(0) = \sigma_{ij}^{c} - \Delta\rho_{ij}^{c}$ and $\sigma_{ij}(\Delta t) = \sigma_{ij}^{c}$. A creep strain $\Delta\varepsilon_{ij}^{c}$ occurs, related to the relaxation of stress $\Delta\rho_{ij}^{c}$ by the equations (18) and (19), i.e.

$$\Delta\varepsilon_{ij}^{Tc\prime} = \frac{1}{2\mu}\Delta\rho_{ij}^{c\prime} + \Delta\varepsilon_{ij}^{c} \tag{23}$$

$$\Delta\varepsilon_{kk}^{Tc} = \frac{1}{3K}\Delta\rho_{kk}^{c} \tag{24}$$

In conformity with the plasticity solution we assume a kinematically constrained solution where the creep strain rate during $t_1 \le t \le t_1 + \Delta t$ remains in a constant tensorial direction, i.e. $\dot{\varepsilon}_{ij}^{c} = \dot{\bar{\varepsilon}}^{c} n_{ij}$ where n_{ij} is a constant tensor. The constitutive relation is assumed to be Norton's law,

$$\dot{\varepsilon}_{ij}^{c} = \frac{3}{2}\frac{\dot{\varepsilon}_0}{\sigma_0^n}\bar{\sigma}^{n-1}\sigma'_{ij}, \quad \text{i.e.} \quad \dot{\bar{\varepsilon}}^{c} = \frac{\dot{\varepsilon}_0}{\sigma_0^n}\bar{\sigma}^{n} \tag{25}$$

where *n* is the creep index of the material, $\dot{\varepsilon}_0$ is the uniaxial steady state creep rate corresponding to temperature θ and uniaxial stress σ_0. Hence σ'_{ij} describes a radial path in deviatoric stress space and $\bar{\sigma}(\dot{\sigma}_{ij}) = \dot{\bar{\sigma}}(\sigma_{ij})$. $\bar{\sigma}$ denotes the von Mises effective stress and $\bar{\varepsilon}$ the von Mises effective strain. During the relaxation process we assume, at each point in space, that an elastic follow-up factor Z exists, i.e. for uni-axial conditions

$$\dot{\varepsilon}^{c} = -\frac{Z}{E}\dot{\sigma} \quad \text{and} \quad \dot{\bar{\varepsilon}}^{c} = -\frac{Z}{\bar{E}}\dot{\bar{\sigma}} \tag{26}$$

for multi-axial conditions where $\bar{E} = \frac{3E}{2(1+\nu)}$.

Combining (25) and (26) and integrating over the relaxation period, we obtain

$$\frac{\dot{\varepsilon}_0 \overline{E}}{\sigma_0^n Z}\Delta t = -\int_0^{\Delta\rho^c} \frac{d\overline{\sigma}}{\overline{\sigma}^n} = \frac{1}{n-1}\left\{\frac{1}{(\sigma^c)^{n-1}} - \frac{1}{(\sigma^c + \Delta\rho^c)^{n-1}}\right\} \tag{27}$$

where $\Delta\rho^c = \overline{\sigma}(\Delta\rho_{ij}^c)$. Integrating (26) gives

$$\overline{\varepsilon}(\Delta\varepsilon_{ij}^c) = \Delta\varepsilon^c = \frac{Z}{\overline{E}}\Delta\rho^c \tag{28}$$

Combining (27) and (28) and eliminating $Z/\overline{E}$ provides an implicit relationship between the effective values σ^c , $\Delta\rho^c$ and $\Delta\varepsilon^c$. Computationally it is advantageous to be able to compute σ^c at each iteration in terms of a fictional rate $\dot{\overline{\varepsilon}}^F$,

$$\sigma^c = \sigma_0\left(\frac{\dot{\overline{\varepsilon}}^F}{\dot{\varepsilon}_0}\right)^{1/n} \tag{29}$$

Combining(27), (28) and (29) gives,

$$\dot{\overline{\varepsilon}}^F = \frac{\Delta\varepsilon^c}{\Delta t} f(\sigma_f, \Delta\rho^c, n) = \frac{\Delta\varepsilon^c}{\Delta t}\left\{\frac{(\sigma^c)^n}{\Delta\rho^c}\frac{1}{n-1}\left\{\frac{1}{(\sigma^c)^{n-1}} - \frac{1}{(\sigma^c + \Delta\rho^c)^{n-1}}\right\}\right\} \tag{30}$$

Hence in the iterative process we begin with current estimates σ^{ci} , $\Delta\rho^{ci}$ and $\Delta\varepsilon^{ci}$ and compute a new value of the creep stress $\sigma^c = \sigma^{cf}$ from (29) where

$$\dot{\overline{\varepsilon}}^F = \frac{\Delta\varepsilon^{ci}}{\Delta t} f(\sigma^{ci}, \Delta\rho^{ci}, n) \tag{31A}$$

Note that in the limit when $\Delta\rho^c/\sigma^c$ is small, $f \to 1$ and

$$\dot{\overline{\varepsilon}}^F = \Delta\varepsilon^c/\Delta t \tag{31B}$$

with an error of the order of $(\Delta\rho^c/\sigma^c)^2$.

9. NUMERICAL EXAMPLE: A PLATE WITH A CENTRAL HOLE AND SUBJECTED TO VARYING THERMAL LOADS AND CONSTANT MECHANICAL LOAD

The geometry of the structure and its finite element mesh are shown in Fig.1, posed as a three dimensional problem. The 20-node solid isoparametric element with reduced integration is adopted. The ratio between the diameter *D* of the hole and the length *L* of the plate is 0.2 and the ratio of the depth of the plate to the length *L* of the plate is 0.05.

The plate is subjected to a temperature difference $\Delta\theta$ between the edge of the hole and the edge of the plate and uniaxial tension *P* acts along one side (Figure 1). The variation of the temperature with radius r was assumed to be;

$$\theta = \theta_0 + \Delta\theta \ln(5a/r)/\ln(5) \tag{32}$$

which gives a simple approximation to the temperature field corresponding to $\theta = \theta_0 + \Delta\theta$ around the edge of the hole and $\theta = \theta_0$ at edge of the plate.

The elastic stress field and the maximum effective value, σ_{t0}, at the edge of the holed plate due to the thermal load was calculated by ABAQUS [20], where $\theta_0 = 0$, $\Delta\theta = 500\ ^\circ C$ and a coefficient of thermal expansion of $10^{-5}\ ^\circ C^{-1}$. The yield stress $\sigma_Y = 360MPa$, and the elastic modulus E = 208 GPa and $\nu = 0.3$. It is coincident that the above calculated σ_{t0} is the reverse plasticity limit, i.e. $\sigma_{t0} = 2\sigma_y$.

For the creep material data in equation (25) we adopt $\sigma_0 = \dfrac{\sigma_y}{2}$, n=5 and

$$\dot{\varepsilon}_0 = 576.53108 \exp\left[\frac{(-19700)}{(\theta + 273)}\right]./\text{hr} \tag{33}$$

where the creep properties depend on temperature, typical of type 316 stainless steel (Table I).

Figure 2 shows the cyclic loading condition. Totally there are two load extremes for this varying thermal loads and constant mechanical load. However, in order to evaluate the creep relaxation in the dwell period Δt, we introduce an extra load instance for assessing this creep behaviour (Figure 3). Hence, we have three load instances in the computation. Instance 1 is for the load extreme 1, i.e. the holed plate subjected to the maximum thermal loads and constant mechanical load. Instance 2 is for the load extreme 1 as well, but used to evaluate the creep relaxation during dwell period. Instance 3 is for the load extreme 2, i.e. the holed plate subjected to the minimum thermal loads and constant mechanical load

Figure 4 shows the shakedown and ratchet boundaries for the problem, using the methods described in [13, 14]. Three load cases are shown in Table II and Fig.4. For load case 1, only cyclic thermal load was applied on the holed plate, where $\theta_0 = 0$, $\Delta\theta = 750\ ^\circ C$. There is no mechanical load and the creep dwell time is 10000 hours. For load case 2, not only the same cyclic thermal loads, but also the mechanical load are applied on the structure, which equals to $0.4\sigma_y$ and the creep

dwell time is 10000 hours. For load case 3, the ratchetting mechanism involves. The same cyclic thermal loads is applied, but the mechanical load is applied on the structure, which equals to $0.5\sigma_y$ and the creep dwell time is 10000 hours

Figure 5-10 present the plastic strain amplitudes at load extremes and the accumulated creep strain after dwell period 10000 hours for the holed plate subjected to three load cases by both the LMM and the step-by-step analyses. It can be seen that the solutions of these strains are near same with or without constant mechanical load. This numerical fact supports the developed creep-reverse plasticity solution method in [15, 16], where only the cyclic loads were considered and the constant loads disappeared in the formulations, i.e. the constant load has little effects on the evaluation of the creep-reverse plasticity mechanism.

The LMM results have a good agreement with ABAQUS step-by-step analysis results, although the value of the effective plastic and creep strains by LMM are slightly higher than those by ABAQUS step-by step analyses. The reason is that in ABAQUS step-by-step analyses, we only calculate 50 load cycles. In order to evaluate the structure at the steady cyclic state, more load cycles need to be performed, which leads to slightly higher values of strains. By the LMM analysis, a steady cyclic state solution can be obtained directly, which produces the less conservative results than R5 method [1]. Figure 11 also produces the contours of effective ratchetting strains over the cycle for three load cases using the Linear Matching method. It is demonstrated again that the ratchet strains in Fig. 11 for three load cases correspond to their load domains in Fig. 4. Only the load case 3 outside the ratchet limit curve in Fig.4 shows significant ratchetting mechanism in Fig.11.

Table III and IV present the comparisons of key parameters of point A and B of the holed plate by LMM and step-by-step analysis. It is verified again that the LMM results have a good agreement with ABAQUS step-by-step solutions. The introduction of the constant mechanical load has little effect on the plastic strain amplitudes and accumulated creep strains at the steady cyclic state. For all three cases, the elastic follow-up factors Z for point A and B are almost same and approximately equals to 2.2. It can also be seen that the summation of the effective plastic strain amplitude at load instance 1 and the effective creep strain over dwell period is approximately equal to the effective plastic strain amplitude at load instance 3. This is a direct and full numerical proof of the creep-reverse plasticity mechanism [16].

By the comparisons of the total number of increments and total CPU time in the ABAQUS analyses (Table V), it can be seen that the time consuming of the step-by-step analysis is more than 20 times of the LMM. This is a main advantage of the simplified method.

Figures 12-17 show the effective steady cyclic stresses at three load instances for the holed plate subjected to three load cases by both the LMM and the step-by-step analyses, respectively. It still can be seen that the LMM results have a good agreement with the ABAQUS step-by-step analyses. Unlike the above magnitude of strains, the solutions of steady cyclic stresses with constant mechanical load are quite different with those without constant mechanical load. However, by the further comparisons of the residual stress amplitudes at three load instances (Fig. 18-20), it can be seen that the inclusive of the constant mechanical load has no effects on these residual stress fields, which determine the plastic strain amplitudes at load instances and the accumulated creep strain over the dwell time.

10. CONCLUSIONS

In this paper, by the extension of previous Linear Matching Method, a new integrity assessment technique is proposed to evaluate plastic and creep behaviours for bodies subjected to cyclic thermal and mechanical loading at a steady cyclic state. The plastic strain range, the accumulated creep strain over dwell period and the ratchetting strain over the cycle are calculated by an iterative process. The constant and varying residual stress fields associated with differing mechanisms as well as the steady cyclic stress state of the whole component are obtained by LMM for the further structural design and assessment.

The LMM assessment procedure in this paper is designed to evaluate the high temperature components subjected to cyclic loading conditions with three or more load instances. Hence this paper provided an important supplement of the previous LMM [12] on the integrity assessment of structures.

By the application of LMM to the holed plate with cyclic thermal loads and constant mechanical load, the solutions in the paper verified the creep-reverse plasticity mechanism and its corresponding assumptions proposed in [15, 16]. It was also demonstrated that the effects of the constant mechanical load on the final creep deformation are insignificant. Although the steady state stresses are quite different between two cases with or without the constant mechanical loads, the varying residual stresses associated with the creep relaxation mechanism are nearly the same.

The FE step-by-step analyses in the paper provide nearly identical solutions with LMM when adopting the same material assumption. However, the time consuming of a typical FE step-by-step analysis is normally more than 20 times of the LMM (Table V). This is a main advantage of the LMM. Another advantage of LMM is that LMM only make use of a standard collection of uniaxial test data without the need for the development of full constitutive descriptions.

The work of this paper is part of a general study of the application of the Linear Matching Method to the various stages of Life Assessment methods, using R5 [1]. It is anticipated that such methods may then provide an alternative to rule-based methods currently used, providing more accurate and less conservative predictions. The form of the method allows it to be implemented in conventional commercial finite element code ABAQUS [20]. This allows the method to become a general purpose method which, unlike most programming methods, does not requires specialist codes.

ACKNOWLEDGEMENTS

The authors gratefully acknowledge the support of the Engineering and Physical Sciences Research Council of the United Kingdom, British Energy Ltd and the University of the Leicester during the course of this work.

REFERENCE

1. Ainsworth RA (editor). R5: Assessment procedure for the high temperature response of structures. *Issue 3*, British Energy Generation Ltd, 2003.
2. Ainsworth RA, Budden PJ. Approximate inelastic analysis of defective components. *Nuclear Engineering and Design* 1992; **133**: 513-523.
3. Marriott DL. Evaluation of deformation or load control of stresses under inelastic conditions using elastic finite element stress analysis. *Proc ASME Pressure Vessels and Piping Conference*. Pittsburgh, Pennsylvania, PVP-136, 1998; 3-9.
4. Seshadri R. The generalised local stress strain (GLOSS) analysis – theory and application. *Trans ASME, J. Pressure Vessel Technology* 1991; **113**: 219-227.
5. Mackenzie D, Boyle JT. A simple method of estimating shakedown loads for complex structures. *Proc ASME Pressure Vessels and Piping Conference*. Denver, PVP-265, 1993; 89-94.

6. Nayebi A, El Abdi R. Cyclic plastic and creep behaviour of pressure vessels under thermomechanical loading. *Computational Materials Science* 2002; **25**: 285-296.
7. Yokobori T, Yokobori A. High temperature creep, fatigue and creep–fatigue interaction in engineering materials. *International Journal of Pressure Vessels and Piping* 2001; **78**: 903-908.
8. Engelhardt MJ. Computation modelling of shakedown. *PhD thesis*, Department of Engineering, University of Leicester, 1999.
9. Ponter ARS, Engelhardt M. Shakedown limits for a general yield condition. *European Journal of Mechanics A/Solids* 2000; **19**: 423-445.
10. Chen HF, Ponter ARS. Shakedown and limit analyses for 3-D structures using the Linear Matching Method. *International Journal of Pressure Vessels and Piping* 2001; **78(6)**: 443-451.
11. Chen HF, Engelhardt MJ, Ponter ARS. Linear matching method for creep rupture assessment. *International Journal of Pressure Vessels and Piping* 2003; **80**: 213-220.
12. Chen HF, Ponter ARS. Application of the Linear Matching Method to the integrity assessment for the high temperature response of structures. *ASME Pressure Vessels and Piping Division (Publication)*, PVP 458, 2003; 3-12.
13. Ponter ARS, Chen HF. A minimum theorem for cyclic load in excess of shakedown, with application to the evaluation of a ratchet limit. *European Journal of Mechanics, A/Solids* 2001; **20 (4)**: 539-553.
14. Chen HF, Ponter ARS. A method for the evaluation of a ratchet limit and the amplitude of plastic strain for bodies subjected to cyclic loading. *European Journal of Mechanics, A/Solids* 2001; **20 (4)**: 555-571.
15. Chen HF, Ponter ARS. Methods for the evaluation of creep relaxation and the amplitude of reverse plastic strain for bodies subjected to cyclic loading. *ASME Pressure Vessels and Piping Division (Publication)*, PVP 459, 2003; 155-164.
16. Chen HF, Ponter ARS. A simplified creep-reverse plasticity solution method for bodies subjected to cyclic loading. *European Journal of Mechanics, A/Solids* 2004; **23**: 561-577.
17. Chow C, Morrison D. Hartlepool/Heysham 1 power stations: behaviour of the superheater header tubeplate beyond global shakedown. *E/EAN/STAN/0012/AGR/01*. British Energy Generation Ltd, 2001.

18. Chen HF, Ponter ARS. Integrity assessment of a 3D tubeplate using the linear matching method: Part 1 Shakedown, reverse plasticity and ratchetting. *International Journal of Pressure Vessels and Piping* 2005; **82(2)**: 85-94.
19. Chen HF, Ponter ARS. Integrity assessment of a 3D tubeplate using the linear matching method: Part 2 Creep relaxation and reverse plasticity. *International Journal of Pressure Vessels and Piping* 2005; **82(2)**: 95-104.
20. ABAQUS. *User's manual*. Version 6.3, 2002.

Table I. Particular functional forms and material coefficients adopted in the paper.

Young's modulus E	Poisson's ratio ν	coefficient of thermal expansion α	Yield stress σ_y	Creep material data $\dot{\varepsilon}_s^c = B.\exp\left[\frac{(-Q)}{(\theta+273)}\right].\bar{\sigma}^n$ (h^{-1})		
				Ln {B}	Q (K)	n
208GPa	0.3	$1.0\times10^{-5}/°C$	360MPa	-19.607755	1.97×10^4	5

Table II. Definition of load domains for the holed plate.

Case	The cyclic thermal load $\Delta\theta$	σ_P	Δt (hours)	Mechanism
Case 1	$1.5\sigma_{t0}\rightarrow 0\rightarrow 1.5\sigma_{t0}\cdots$	0	10000	Reverse plasticity
Case 2	$1.5\sigma_{t0}\rightarrow 0\rightarrow 1.5\sigma_{t0}\cdots$	$0.4\sigma_y$	10000	Reverse plasticity
Case 3	$1.5\sigma_{t0}\rightarrow 0\rightarrow 1.5\sigma_{t0}\cdots$	$0.5\sigma_y$	10000	Ratchetting

Table III. Comparison of key parameters of point A by LMM and step-by-step analysis.

Case	Method	$\Delta\bar{\rho}_c$ (MPa)	$\Delta\bar{\varepsilon}_c$ (Δt=10000h)	Z	$\Delta\bar{\varepsilon}_p$ at load instance 1	$\Delta\bar{\varepsilon}_p$ at load instance 3	Ratchetting strain per cycle
Case 1	LMM	296.318	2.810×10^{-3}	2.276	3.355×10^{-3}	6.235×10^{-3}	1.457×10^{-4}
	Step-by-step	287.225	2.656×10^{-3}	2.219	3.354×10^{-3}	6.056×10^{-3}	1.094×10^{-4}
Case 2	LMM	295.241	2.817×10^{-3}	2.290	3.505×10^{-3}	6.326×10^{-3}	1.047×10^{-4}
	Step-by-step	287.454	2.652×10^{-3}	2.214	3.353×10^{-3}	6.064×10^{-3}	1.159×10^{-4}
Case 3	LMM	295.932	2.808×10^{-3}	2.277	3.485×10^{-3}	8.371×10^{-3}	2.196×10^{-3}
	Step-by-step	289.897	2.658×10^{-3}	2.201	3.358×10^{-3}	7.684×10^{-3}	1.758×10^{-3}

Table IV. Comparison of key parameters of point B by LMM and step-by-step analysis.

Case	Method	$\Delta\overline{\rho}_c$ (MPa)	$\Delta\overline{\varepsilon}_c$ (Δt=10000h)	Z	$\Delta\overline{\varepsilon}_p$ at load instance 1	$\Delta\overline{\varepsilon}_p$ at load instance 3	Ratchetting strain per cycle
Case 1	LMM	296.312	2.812×10^{-3}	2.277	3.352×10^{-3}	6.233×10^{-3}	1.460×10^{-4}
	Step-by-step	287.238	2.656×10^{-3}	2.219	3.353×10^{-3}	6.054×10^{-3}	1.093×10^{-4}
Case 2	LMM	296.02	2.809×10^{-3}	2.277	3.373×10^{-3}	6.232×10^{-3}	1.358×10^{-4}
	Step-by-step	287.049	2.660×10^{-3}	2.224	3.353×10^{-3}	6.040×10^{-3}	1.001×10^{-4}
Case 3	LMM	296.43	2.807×10^{-3}	2.273	3.181×10^{-3}	5.928×10^{-3}	1.147×10^{-4}
	Step-by-step	289.146	2.642×10^{-3}	2.193	3.182×10^{-3}	5.829×10^{-3}	0.918×10^{-4}

Table V. Comparison of computing cost by LMM and step-by-step analysis.

Case	Method	Total number of steps in ABAQUS	Total number of increments in ABAQUS	Total CPU time in ABAQUS (s)
Case 1	LMM	1	75	1323
	Step-by-step	150 (50 load cycles)	2111	45324
Case 2	LMM	1	147	2765
	Step-by-step	150 (50 load cycles)	2154	47016
Case 3	LMM	1	202	3679
	Step-by-step	150 (50 load cycles)	2208	50615

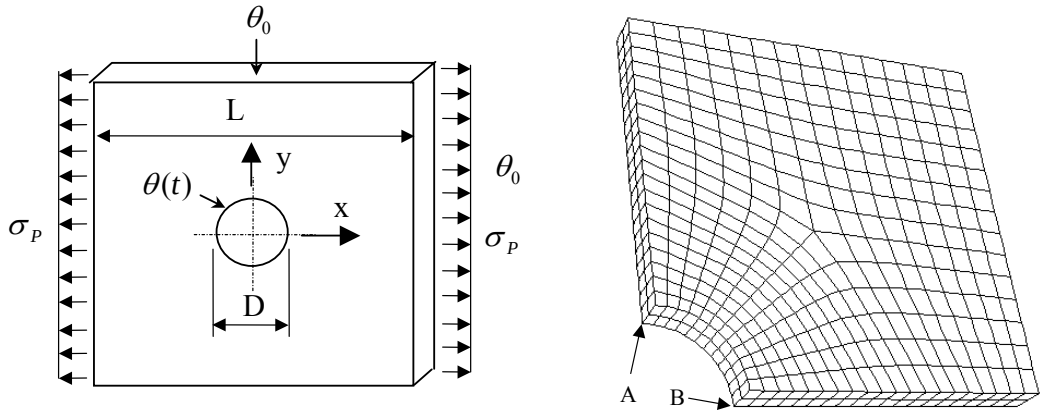

Figure 1. Geometry of the holed plate subjected to varying thermal loads and its finite element mesh (D/L=0.2), the yield stress $\sigma_Y = 360MPa$, the elastic modulus $E = 208GPa$.

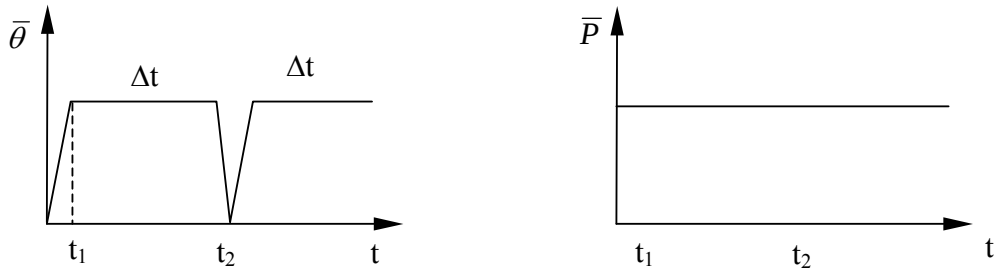

Figure 2. Load history with two distinct extremes (three load instances) to the elastic solution.

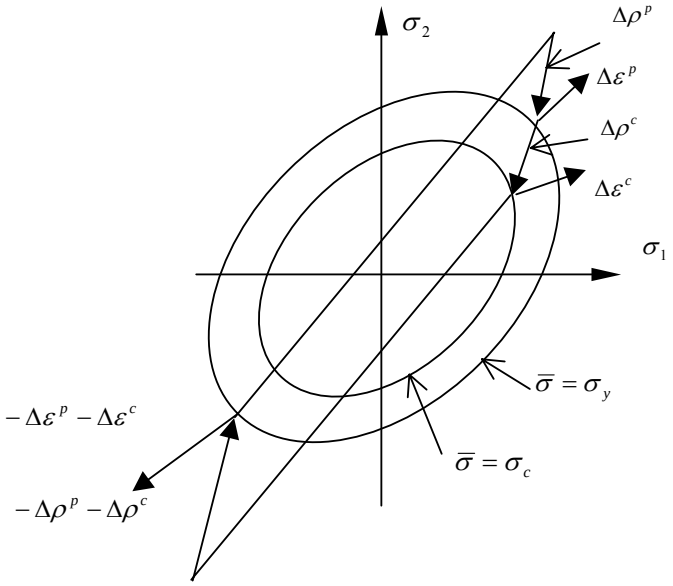

Figure 3. Schematic representation of the quantities for three load instances.

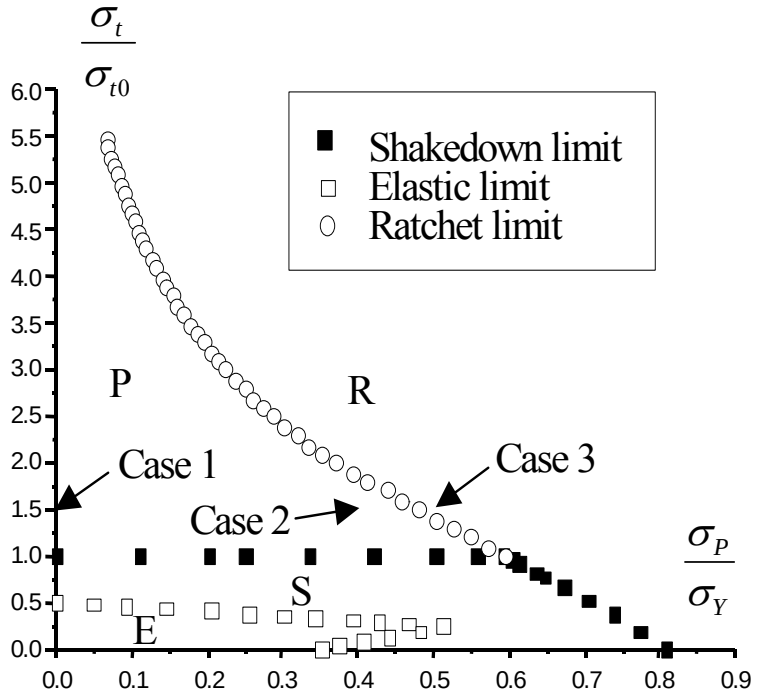

Figure 4. Elastic, shakedown, reverse plasticity and ratchet region for the holed plate with constant mechanical and varying thermal loading.

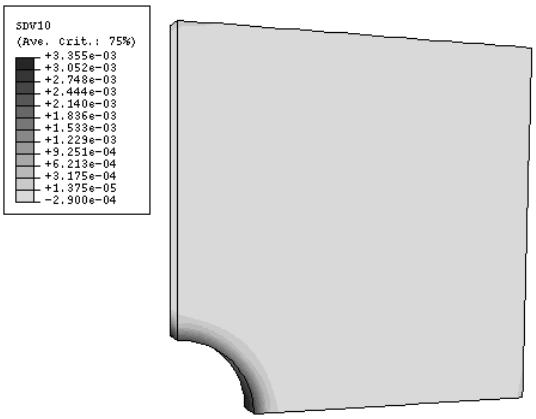

(a) $\sigma_P = 0$

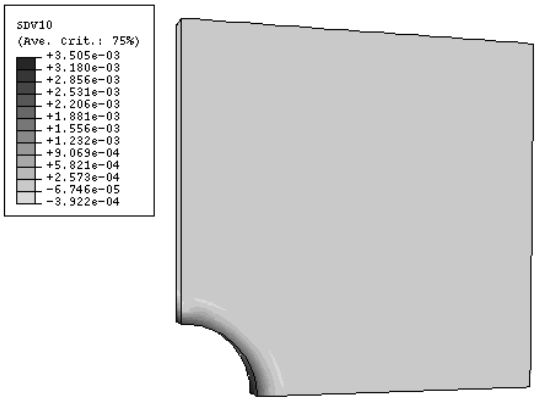

(b) $\sigma_P = 0.4\sigma_y$

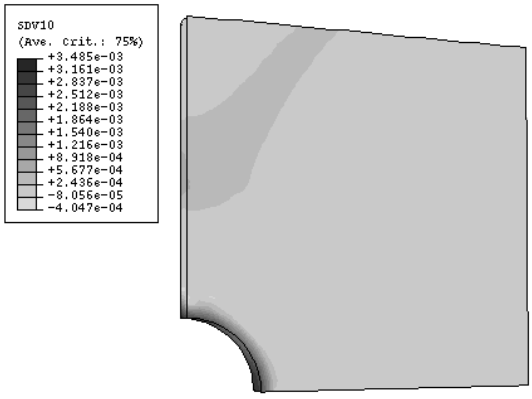

(c) $\sigma_P = 0.5\sigma_y$

Figure 5. Effective plastic strain amplitude at load instance 1 by LMM.

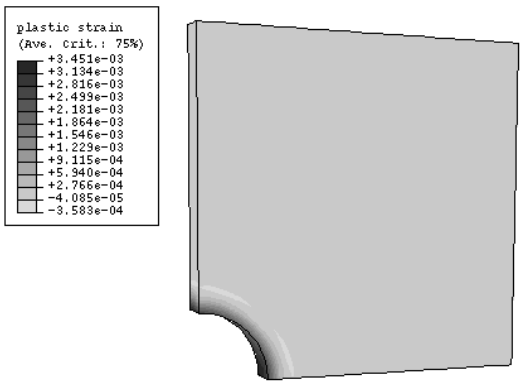

(a) $\sigma_P = 0$

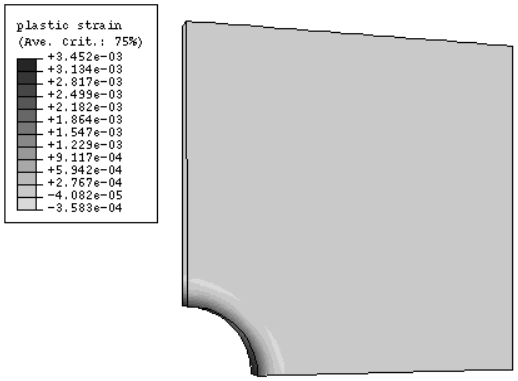

(b) $\sigma_P = 0.4\sigma_y$

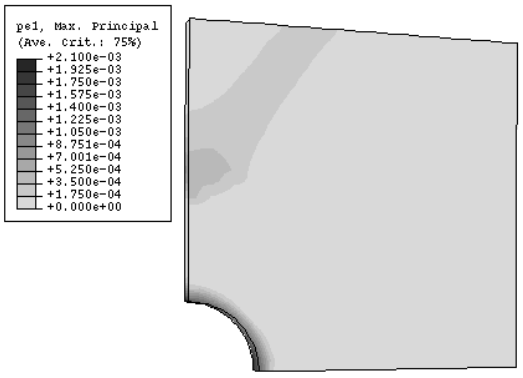

(c) $\sigma_P = 0.5\sigma_y$

Figure 6. Effective plastic strain amplitude at load instance 1 after 50 load cycles by step-by-step analysis.

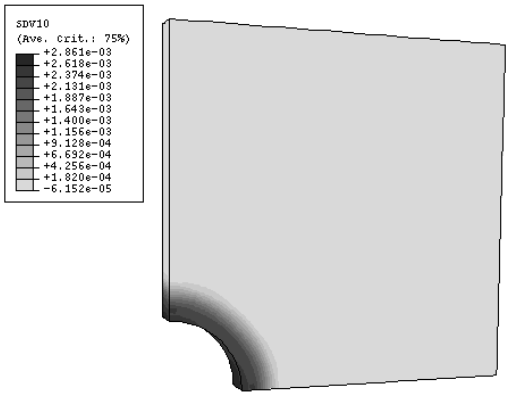

(a) $\sigma_P = 0$

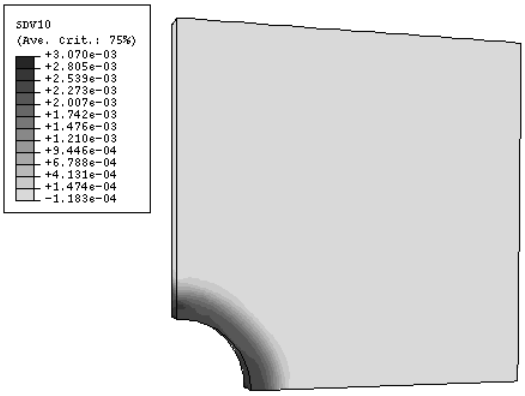

(b) $\sigma_P = 0.4\sigma_y$

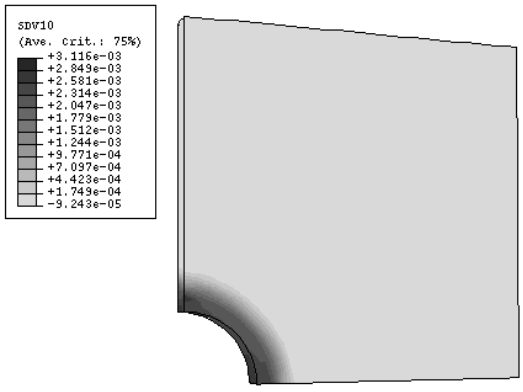

(c) $\sigma_P = 0.5\sigma_y$

Figure 7. Contour of accumulated creep strain at load instance 2, i.e. after dwell period ($\Delta t = 10000h$) by LMM.

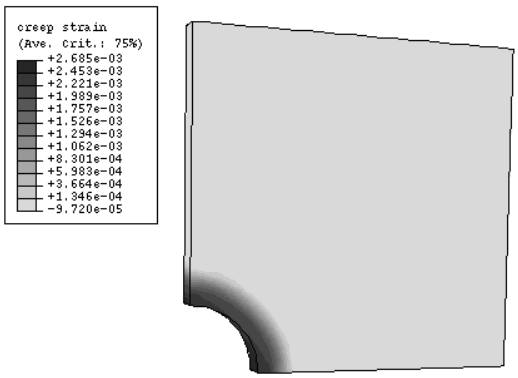

(a) $\sigma_P = 0$

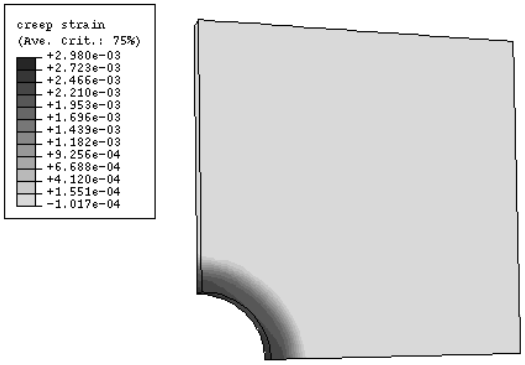

(b) $\sigma_P = 0.4\sigma_y$

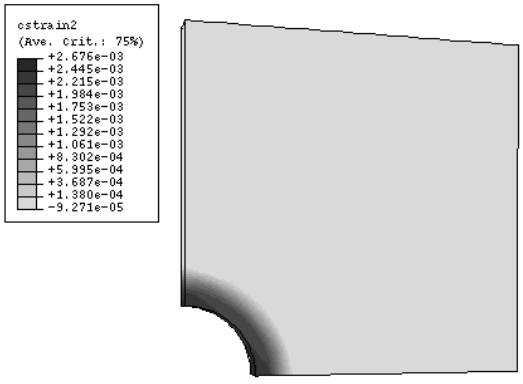

(c) $\sigma_P = 0.5\sigma_y$

Figure 8. Contour of accumulated creep strain at load instance 2, i.e. after dwell period ($\Delta t = 10000h$) after 50 load cycles by step-by-step analysis.

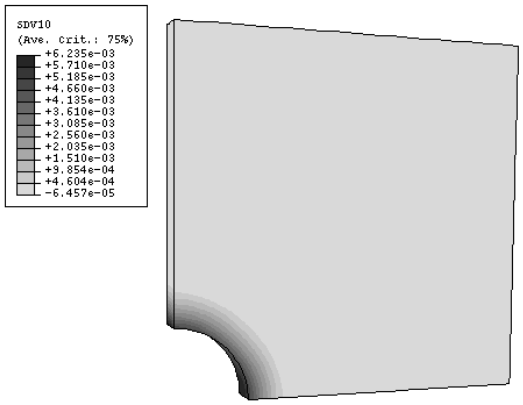

(a) $\sigma_P = 0$

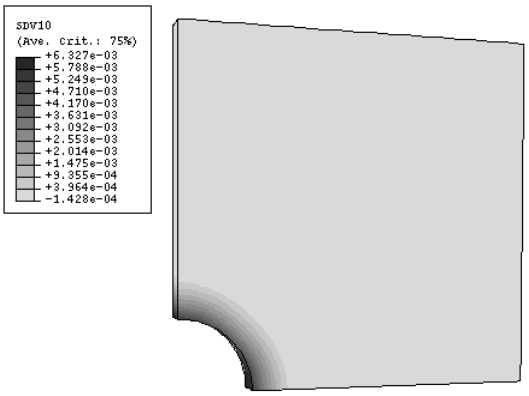

(b) $\sigma_P = 0.4\sigma_y$

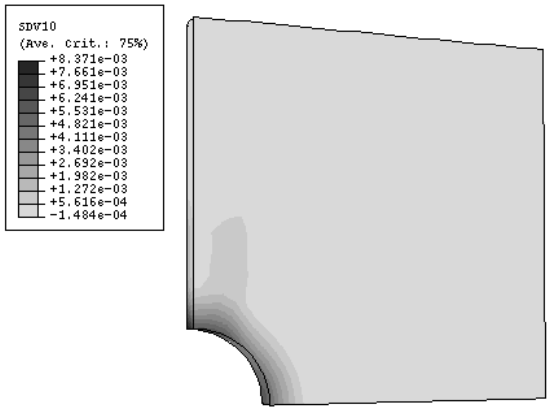

(c) $\sigma_P = 0.5\sigma_y$

Figure 9. Contour of plastic strain amplitude at load instance 3 by LMM.

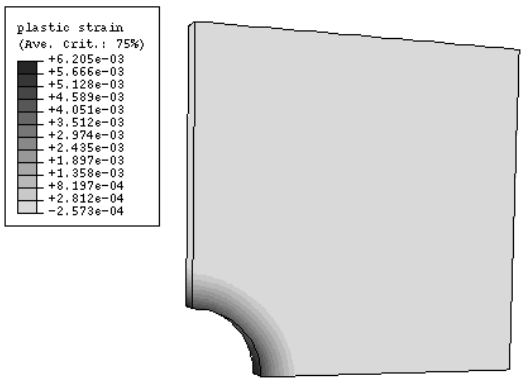

(a) $\sigma_P = 0$

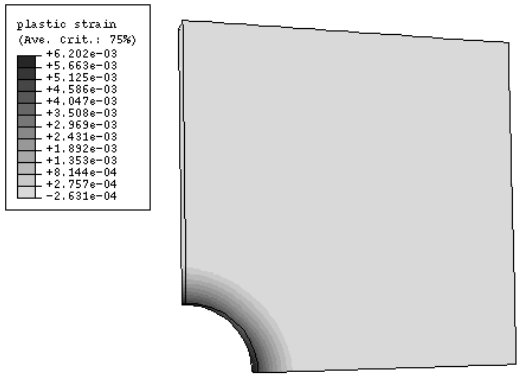

(b) $\sigma_P = 0.4\sigma_y$

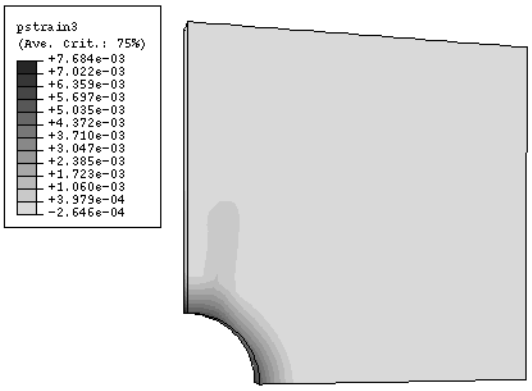

(c) $\sigma_P = 0.5\sigma_y$

Figure 10. Effective plastic strain amplitude at load instance 3 after 50 load cycles by step-by-step analysis.

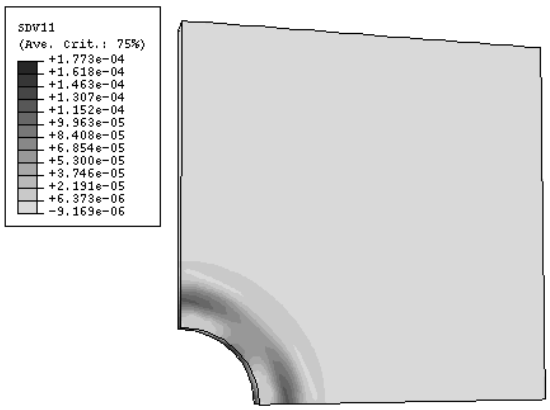

(a) $\sigma_P = 0$

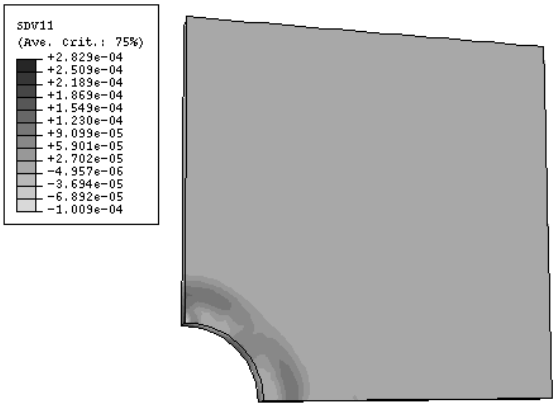

(b) $\sigma_P = 0.4\sigma_y$

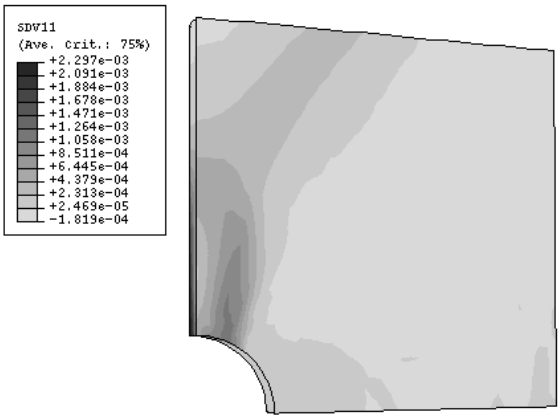

(c) $\sigma_P = 0.5\sigma_y$

Figure 11. Contour of effective ratchetting strain over the cycle by LMM.

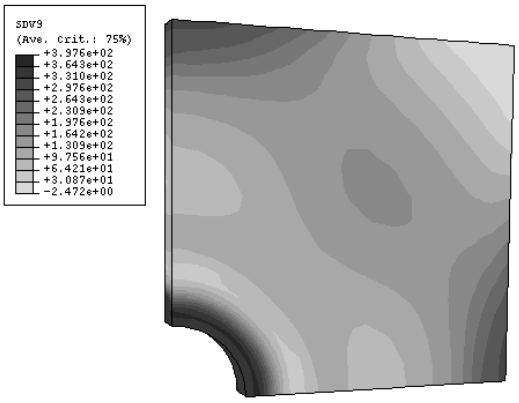

(a) $\sigma_P = 0$

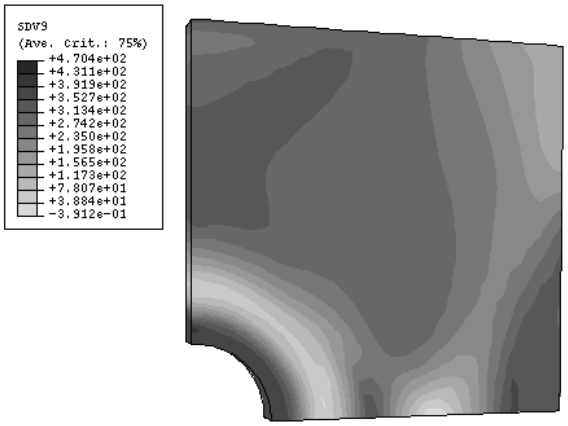

(b) $\sigma_P = 0.4\sigma_y$

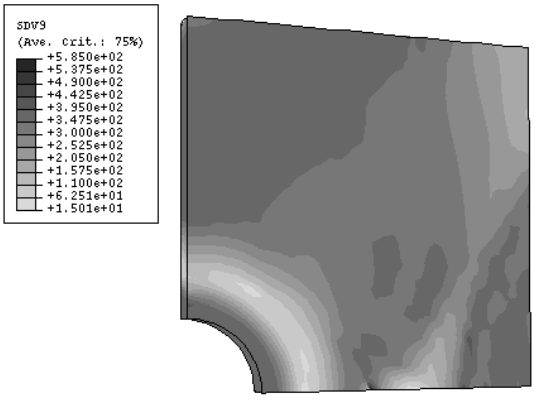

(c) $\sigma_P = 0.5\sigma_y$

Figure 12. Effective steady cyclic stress at load instance 1 by LMM.

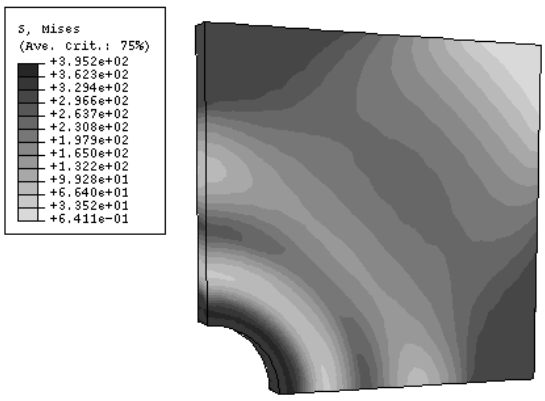

(a) $\sigma_P = 0$

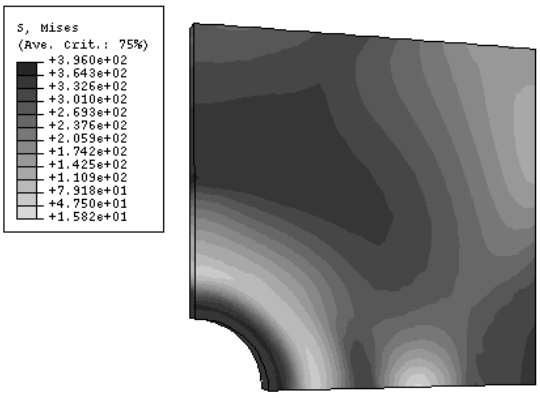

(b) $\sigma_P = 0.4\sigma_y$

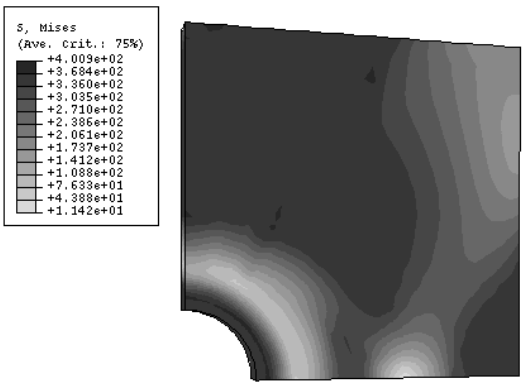

(c) $\sigma_P = 0.5\sigma_y$

Figure 13. Effective steady cyclic stress at load instance 1 after 50 load cycles by the step-by-step analysis.

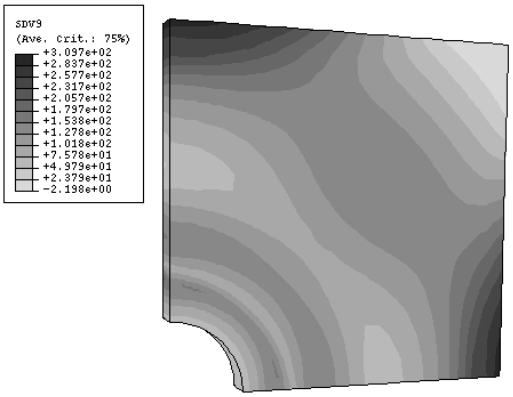

(a) $\sigma_P = 0$

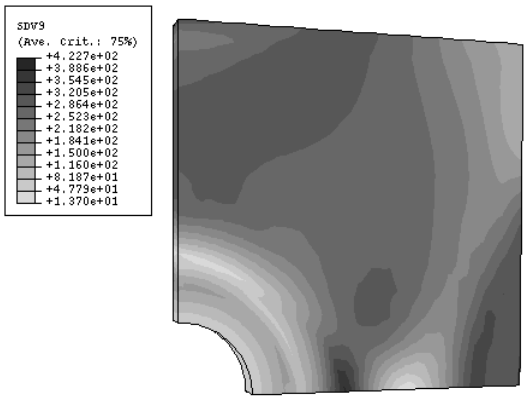

(b) $\sigma_P = 0.4\sigma_y$

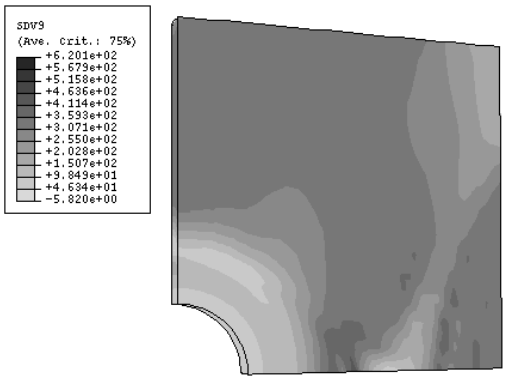

(c) $\sigma_P = 0.5\sigma_y$

Figure 14. Effective steady cyclic stress at load instance 2, i.e. after dwell period ($\Delta t = 10000h$) by LMM.

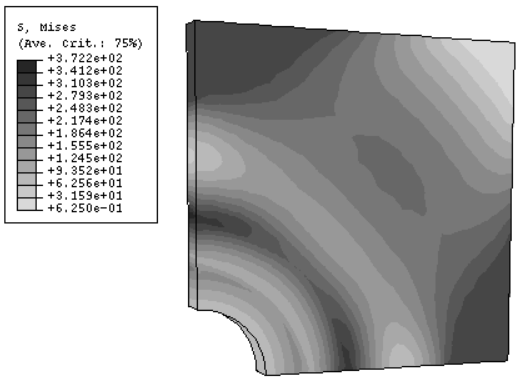

(a) $\sigma_P = 0$

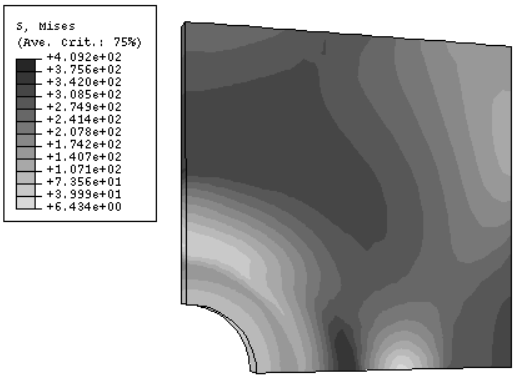

(b) $\sigma_P = 0.4\sigma_y$

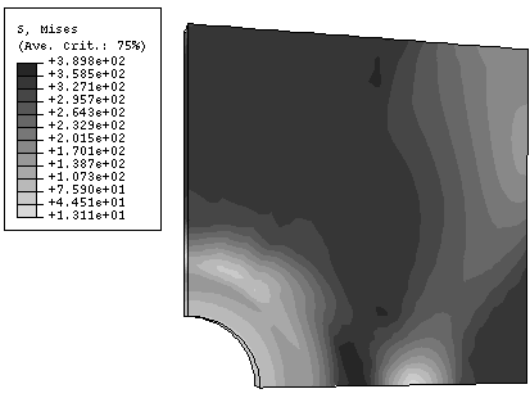

(c) $\sigma_P = 0.5\sigma_y$

Figure 15. Effective steady cyclic stress at load instance 2, i.e. after dwell period ($\Delta t = 10000h$) after 50 load cycles by the step-by-step analysis.

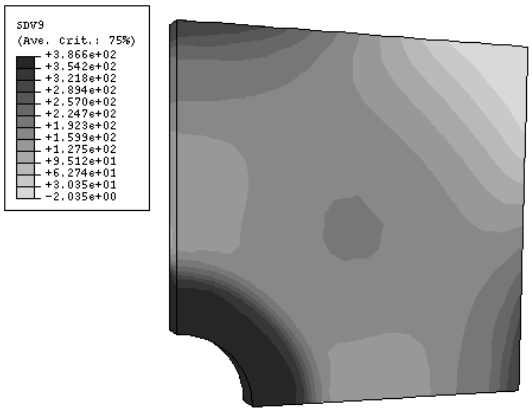

(a) $\sigma_P = 0$

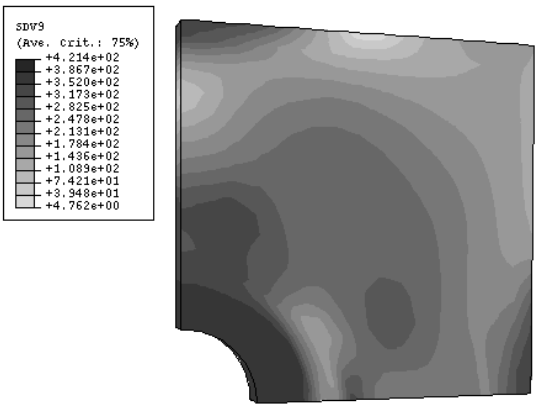

(b) $\sigma_P = 0.4\sigma_y$

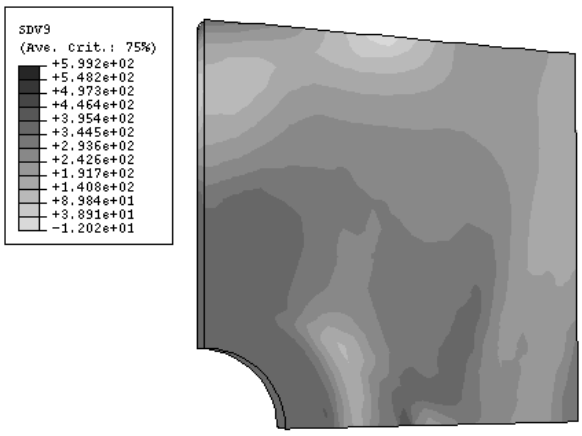

(c) $\sigma_P = 0.5\sigma_y$

Figure 16. Effective steady cyclic stress at load instance 3 by LMM.

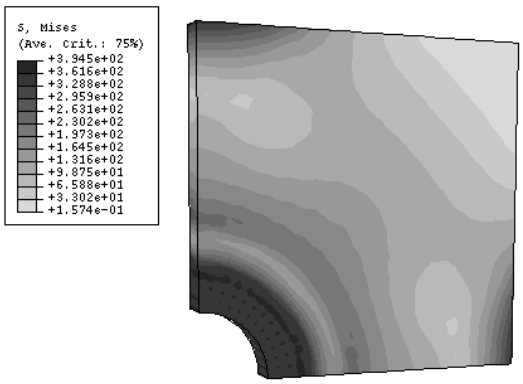

(a) $\sigma_P = 0$

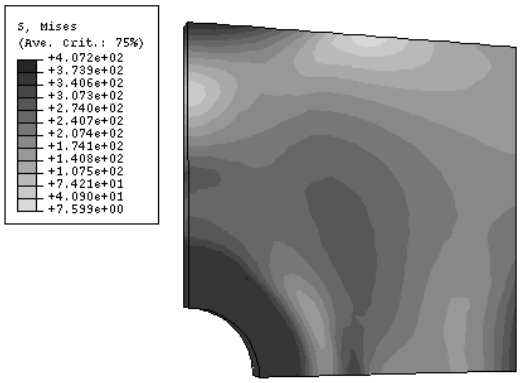

(b) $\sigma_P = 0.4\sigma_y$

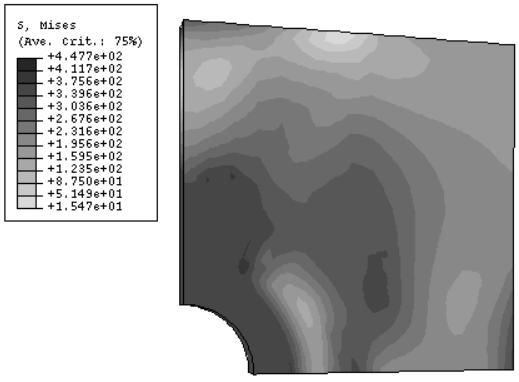

(c) $\sigma_P = 0.5\sigma_y$

Figure 17. Effective steady cyclic stress at load instance 3 after 50 load cycles by the step-by-step analysis.

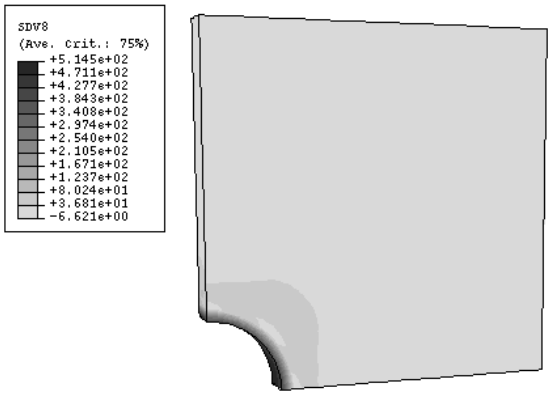

(a) $\sigma_P = 0$

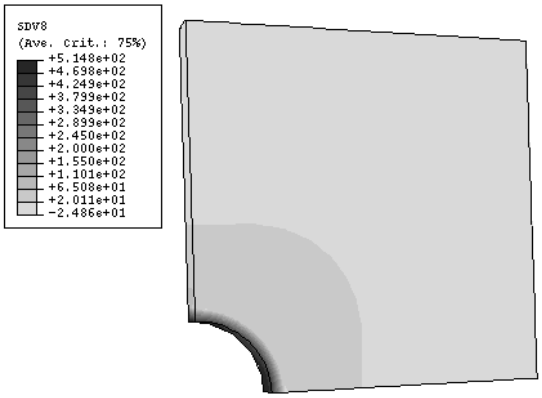

(b) $\sigma_P = 0.4\sigma_y$

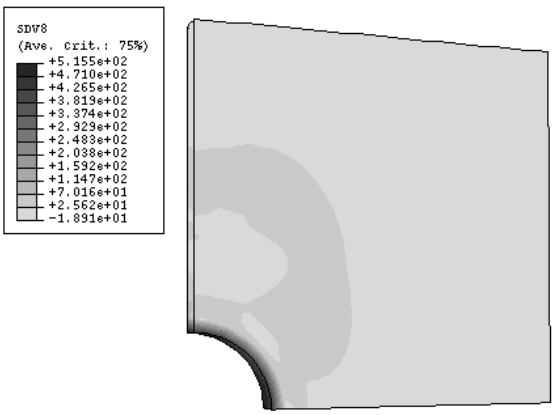

(c) $\sigma_P = 0.5\sigma_y$

Figure 18. Effective residual stress field at load instance 1.

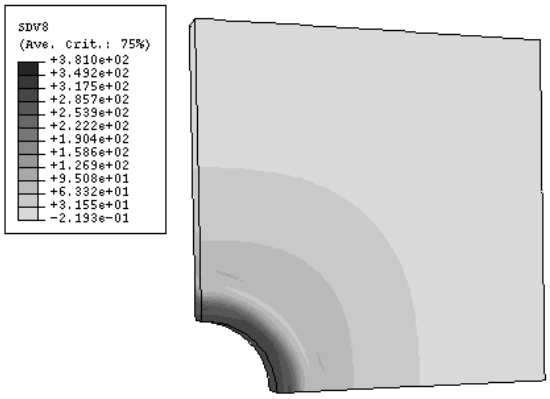

(a) $\sigma_P = 0$

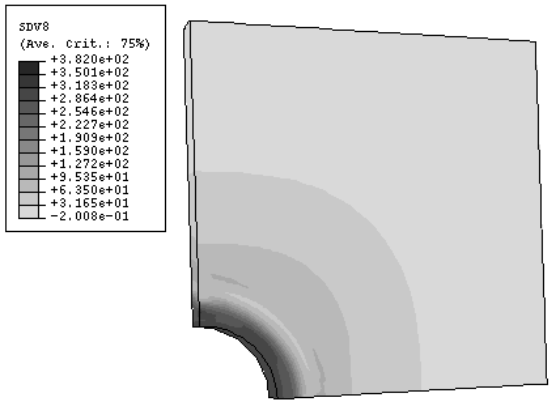

(b) $\sigma_P = 0.4\sigma_y$

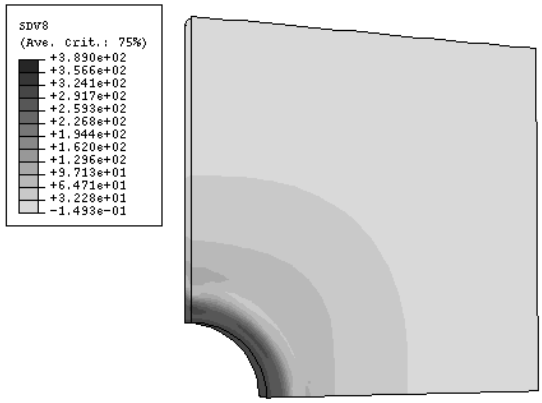

(c) $\sigma_P = 0.5\sigma_y$

Figure 19. Effective residual stress field at load instance 2 associated with creep relaxation.

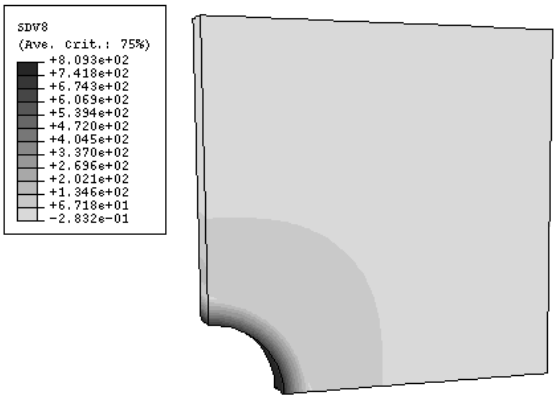

(a) $\sigma_P = 0$

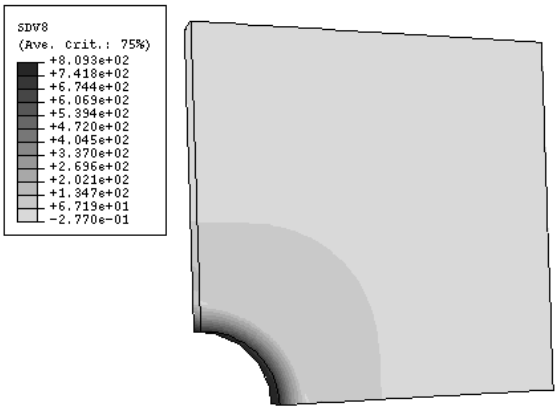

(b) $\sigma_P = 0.4\sigma_y$

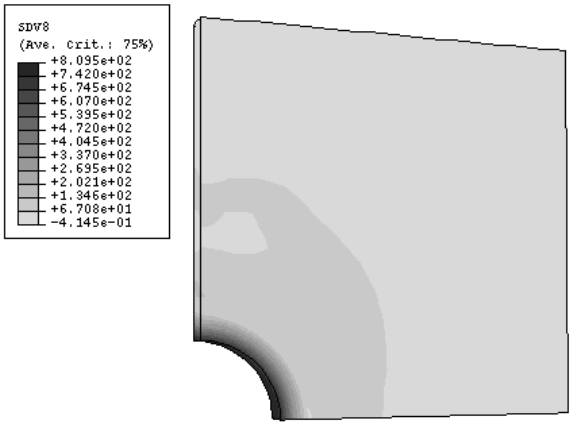

(c) $\sigma_P = 0.5\sigma_y$

Figure 20. Effective residual stress field at load instance 3.